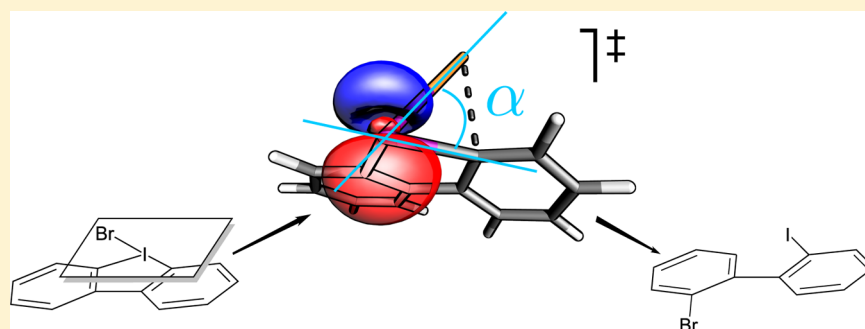


Breaking Down the Reactivity of λ^3 -Iodanes: The Impact of Structure and Bonding on Competing Reaction Mechanisms

Halua Pinto de Magalhães, Hans Peter Lüthi,* and Antonio Togni

Department of Chemistry and Applied Biosciences, ETH Zürich, Vladimir-Prelog-Weg 2, 8093 Zürich, Switzerland

S Supporting Information



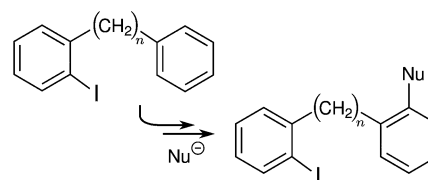
ABSTRACT: The functionalization of arenes via diaryliodonium salts has gained considerable attention in synthesis, as these compounds react under mild conditions. Mechanistic studies have shown that the formation of corresponding λ^3 -iodane intermediates takes a key role, as they determine the course and selectivity of the reaction. Bridged diaryliodonium salts, featuring a heterocyclic moiety involving the iodine atom, were shown to exhibit a distinctly different reactivity, leading to different products. These products are not just the result of reductive elimination reactions but may also arise via radical mechanisms. Our quantum chemical calculations reveal that the λ^3 -iodane intermediate is also the “gateway” for reactions that are observed only for strained bridged systems. At the same time, we find a remarkable affinity of the hypervalent region to planarity for all reaction mechanisms. This also explains the correlation between the size of the bridge connecting the aryl groups and the reaction products observed. Furthermore, the energetics of these competing reactions are examined by analysis of the mechanisms. Finally, using model compounds, some of the basic features governing the reactivity of λ^3 -iodanes are discussed.

INTRODUCTION

Hypervalent iodine compounds are very useful for many organic transformations, both as reagents for a variety of functionalizations and as catalysts for oxidative reactions.^{1–3} Diaryliodonium salts, in particular, are versatile reagents for a number of arylation reactions (see, e.g., ref 4). In the case of diaryliodonium salts containing two different aryl groups, selectivity issues arise as to which group will be transferred to a nucleophile. Our previous corresponding computational study revealed that the partial charge of the ipso carbon atom of the group involved in the hypervalent interaction is a determining factor.⁵ A further interesting, and to some extent unique, class of diaryliodonium salts is that having the two aryl groups either directly connected or bridged by a short alkyl chain, thus forming cyclic derivatives (Scheme 1).⁶ We analyze herein the influence of the ring size on the structure and reactivity of such compounds.

Hypervalence: Conceptual Considerations. The concept of hypervalence applies to main-group p-block elements (groups 13–18) exceeding eight electrons in their valence shell, thus violating the Lewis octet rule (see, e.g., ref 7). As a consequence, molecules containing hypervalent centers exhibit different types of bonding, resulting in often distinct chemical behavior.

Scheme 1. Functionalization of Diarylalkanes under Mild Conditions via a Cyclic Intermediate Diaryliodonium Species



According to Musher,⁸ hypervalent molecules can be divided into two classes: The first type (HV_I), referred to as molecules made out of molecules, consists of systems forming three-center–four-electron (3c–4e) bonds without further rehybridization of the hypervalent center (e.g., SCl₄, IF₃). On the other hand, the HV_{II} class molecules are highly symmetric species involving additional s-electrons in the hypervalent bonds (e.g., XeO₄, PF₅, IF₇). This classification is still the subject of ongoing debate.^{9–11}

Received: July 28, 2014

Published: August 11, 2014

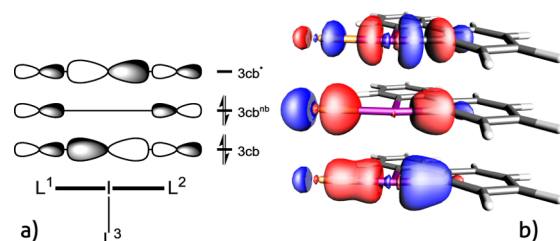
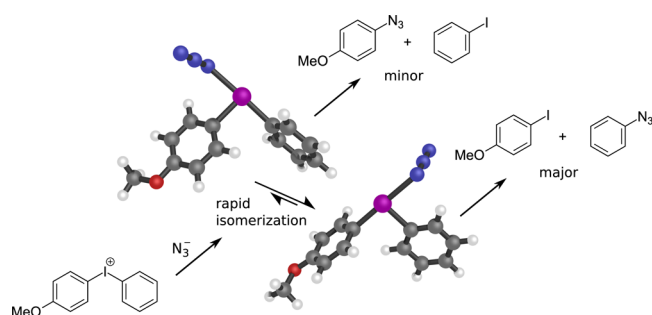


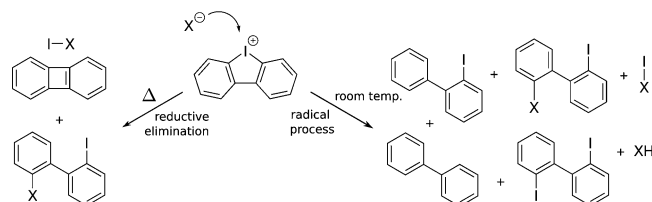
Figure 1. Schematic representation of the three-center–four-electron bond in λ^3 -iodanes (a) along with the corresponding natural localized molecular orbitals (NLMOs) of bromo 1,1'-biphenyl iodane (b). The orbitals are labeled as three-center bonds (3cb) of bonding, nonbonding (nb), or antibonding (*) character.

Scheme 2. Conversion of a Diaryliodonium Salt with an Azide Resulting in the Selective Functionalization of the Phenyl Group via Rapid Isomerization of the Iodane Intermediates^a



^aAll reaction products are the result of a reductive elimination.⁵

Scheme 3. Diaryliodonium Salts with Bridged Ligands (1,1'-Biphenyl Iodonium) Convert to Different Products Depending on the Reaction Conditions^a



^aThe RE leads to functionalization as well as arene coupling products. In addition, products of radical reactions are also observed.

The observation that the most electron-withdrawing substituents are found in mutual *trans* positions in a hypervalent compound, as it is typically observed for λ^3 -iodanes, can be explained by the 3c–4e bond model.^{2,12} The three molecular orbitals describing the 3c–4e interaction show bonding, nonbonding, and antibonding character. The two

lower-energy MOs are occupied by two electrons each (Figure 1). In principle, the 3c–4e bond is delocalized over the three centers, but due to the node at the iodine center in the nonbonding MO, it is highly polarized toward the ligands. Electron-withdrawing ligands at both ends of the three-center bond will therefore stabilize this bonding pattern.⁵

Reactivity and Reaction Patterns. In a previous study, we focused on understanding the selectivity of functionalization starting from diaryliodonium salts (Scheme 2).⁵ Upon addition of the designated nucleophile, these reagents form λ^3 -iodane intermediates that subsequently undergo a selective reductive elimination (RE) under mild conditions. It was demonstrated and confirmed by other groups¹³ that the selectivity is governed by the polarity of the 3c–4e bond, which is predetermined by introducing specific directing groups. In addition, the selectivity can be influenced by the introduction of bulky ligands.¹⁴

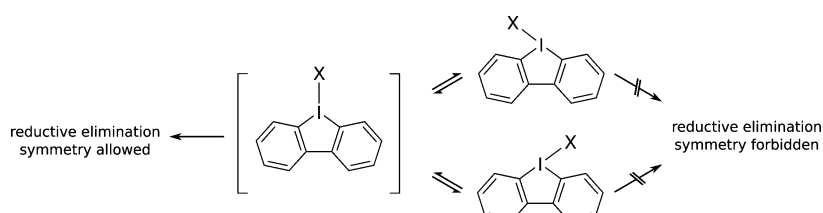
However, totally different reaction patterns are observed using rigid systems such as cyclic diaryliodonium ions (Scheme 3).⁶ The heterocycle can be viewed as consisting of a iodine center bearing bridged ligands. (This is more in line with the transition metal-like aspect of hypervalent iodanes.) Even though this heterocycle shows no aromaticity, bridged diaryliodonium ions are poorly reactive. Considering the conversion with the same nucleophile under similar conditions, the ring systems tend to undergo a radical reaction rather than a reductive elimination reaction as observed for unbridged compounds. However, with increasing heterocycle ring size, the observed reactivity becomes more and more equal to that of the corresponding unbridged systems.

Grushin proposed that conformational nonrigidity is the key factor determining the difference in reactivity.⁶ He also presented a tentative mechanistic explanation to account for the experimental observations. Accordingly, the conversion of bridged diaryliodonium salts with nucleophiles first leads to the formation of a T-shaped hypervalent iodine intermediate, which is able to isomerize to a higher-energy Y-shaped geometry (Scheme 4). In order to follow a symmetry-allowed mechanism, the subsequent reductive elimination reaction has to start from such a Y-shaped configuration. Consequently, the reaction outcome depends on the accessibility of the Y-isomer, which is again dependent on the size of the heterocycle. The reactivity would therefore be determined by the heights of the isomerization and the homolytic decomposition barriers.

COMPUTATIONAL DETAILS

The ab initio computations for this work were performed with the quantum chemical package Gaussian 09 (G09 Rev A.02).¹⁵ Natural localized molecular orbitals (NLMOs) were obtained from the natural bond orbitals (NBOs) using the NBO program, version 3.1.¹⁶ All ground-state geometries were optimized for closed shell singlet states by means of density functional theory (DFT). The B3LYP exchange-correlation functional^{17–20} was employed along with the aug-cc-pVDZ-PP basis sets²¹ (and aug-cc-pVTZ-PP for the IH₃ model

Scheme 4. RE Reaction Involving Bridged Diaryliodonium Salts as Proposed by Grushin⁶



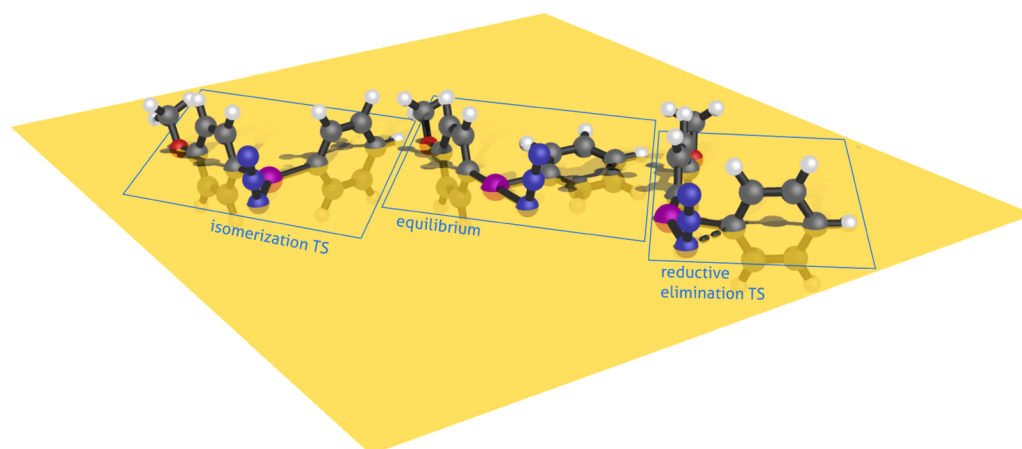


Figure 2. Illustration of the planarity retention of the hypervalent region in the course of the reaction shown in Scheme 2. The plane (in yellow) is defined by the three ipso atoms coordinated to the iodine center. Displayed are the geometries of the isomerization TS, of the intermediate (equilibrium), and of the TS of a RE reaction.

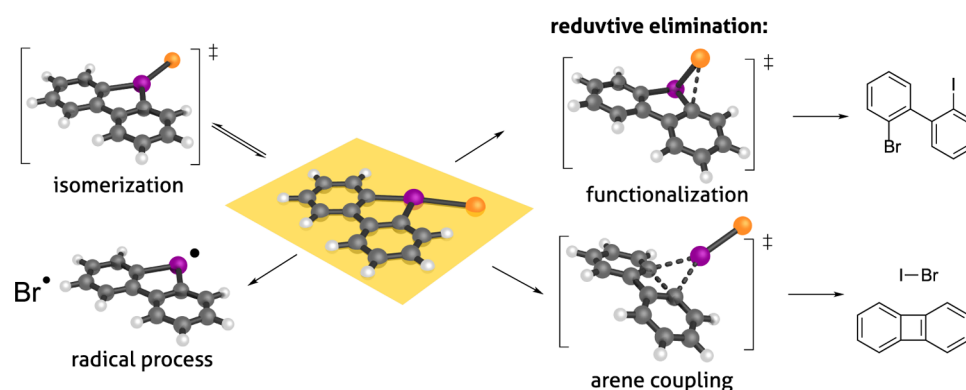


Figure 3. Possible reaction pathways starting from the hypervalent intermediate bromo 1,1'-biphenyl iodane. The preference for a certain reaction pathway depends on the reaction conditions as well as on the bridge size. Obviously, the iodane intermediate is acting in situ as a specific example.

systems). Scalar relativistic and scalar spin-orbit effects were considered for the iodine atom by use of a semilocal electron core potential, the Stuttgart-Koeln-MCDHF-RSC-28-ECP.²² Excited-state energies were obtained by time-dependent DFT^{23–25} with the same functional and basis sets. All energies are given as approximate Gibbs free energies at a temperature of 298.15 K and standard conditions.

RESULTS AND DISCUSSION

Reactions with Bridged Iodanes. As long as no bulky arene ligands are involved, the reaction of a diaryliodonium cation with a nucleophile is well-described by a Curtin-Hammett reaction profile, showing a rapid equilibrium between two iodane isomers and the rate-determining barriers for reductive elimination.⁵ Inspection of the mechanistic features reveals that the hypervalent region, which is constituted by the iodine center and its three immediate bonding partner atoms, thus coinciding with the main molecular plane, preserves planarity throughout the entire reaction. Not only does the isomerization, which occurs via a planar Y-shaped transition structure, follow a planar reaction pathway but also the reductive elimination (Figure 2).

Thanks to their rigid geometry, bridged diaryliodanes, on the other hand, are suited systems to study the impact of a forced deviation from planarity of the hypervalent region. The bridge between the aryl ligands restricts certain degrees of freedom for the possible reaction pathways. Obviously, with the ring size being a tunable parameter, this restriction will vary with the size

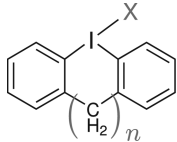
of the bridge. Figure 3 depicts the calculated stationary points of the reaction pathways of the five-membered ring system, starting from a bromo bisphenyl iodane intermediate formed in situ as a specific example.

Figure 3 shows that, in contrast to most unbridged iodanes, the elimination of the original iodonium ligands becomes accessible. The product of interest in this case is biphenylene, which is denoted in the following as the arene coupling product in order to distinguish it from the functionalization product. Besides the two reductive elimination reactions, the iodane intermediate is able to isomerize and react via a competitive radical process.

From Figure 3, it is apparent that both transition-state geometries for the reductive elimination reactions strongly deviate from the essentially planar structure of the intermediate. This is evidently a consequence of the strained ring system, which makes the intramolecular approach to the ipso carbon more difficult. The result is an energy penalty for the corresponding reaction barriers. The computations further confirmed that decreasing the strain in the system by enlarging the ring size has a considerable effect on the barriers of the reductive elimination reactions (Table 1). This is in agreement with the experimental observations reported by Grushin.⁶

Figure 4a shows the barriers for the three reactions (isomerization, functionalization, i.e., aryl-nucleophile coupling, and aryl-aryl coupling) of bridged bromo diaryliodanes as a function of the bridge size. Evidently, the isomerization reaction

Table 1. Barriers of the Competing Reaction Pathways (in kcal/mol) of a Series of Bridged Diaryliodanes as a Function of the Bridge Size n



X	n	0	1	2	3	no bridge
N3	isom.	14.0	11.6	11.5	10.1	11.0
	func.	29.4	22.5	18.0	14.5	13.3
	coupl.	47.7	27.2	19.7	21.1	29.2
Br	isom.	13.8	10.9	10.6	9.6	9.5
	func.	33.3	26.3	21.2	18.1	16.3
	coupl.	48.9	27.4	19.6	21.3	28.6
Ph	isom.	29.2				20.2
	func.	56.0	40.7	34.0	25.4	19.4
	coupl.	30.8	21.2	18.7	17.6	21.4
PFPh ^a	isom.	21.1	16.8	17.6	15.3	14.8
	func.	37.4	31.2	29.1	25.1	21.5
	coupl.	36.3	23.2	19.5	19.5	24.2

^aPentafluorophenyl.

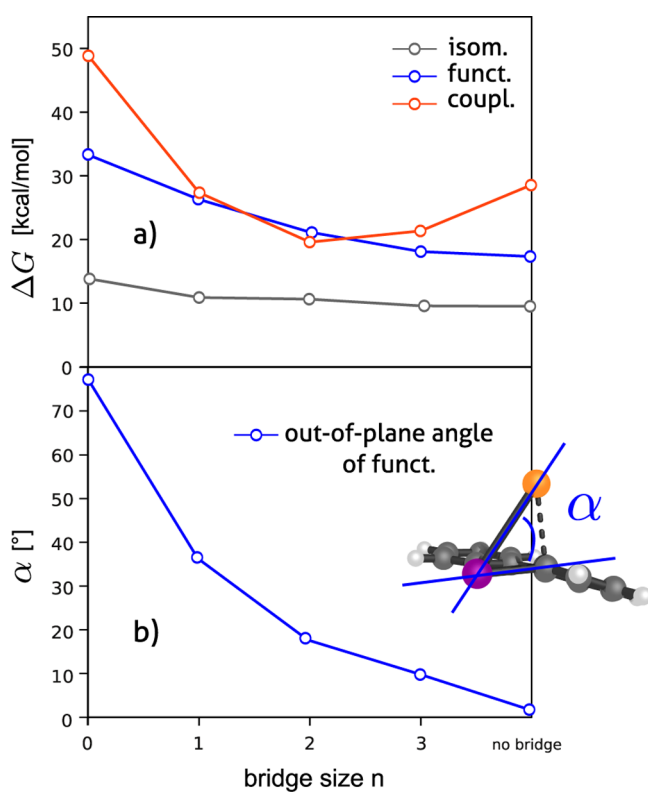


Figure 4. (a) Reaction barriers of the bromo diaryliodane series. Remarkably, the arene coupling has a minimum at the bridge size of $n = 2$ and is favored over the functionalization as well (also, compare to Table 1). (b) Out-of-plane angle α in the TS of the functionalization reaction of the same series.

(gray line in Figure 4a) is not significantly influenced by the ring size. On the other hand, the barriers of the reductive elimination reactions respond strongly to the ring size (blue and red lines, Figure 4a). First, the functionalization barrier (blue line) steadily decreases from over 30 kcal/mol to less than 20 kcal/mol for large bridge sizes. Second, the arene

coupling reaction is competitive only for ring sizes 6–8 (or bridge size $n = 1–3$), from where its barrier will increase again. This explains why the arene coupling reaction is not usually observed in reactions involving unbridged diaryliodanes.

The above-mentioned deviation from coplanarity of the iodine atom and its immediate bonding partners in the transition state may be defined by the angle α between the I–X vector and the plane containing the iodine atom and its two carbon bonding partners. As shown in Figure 4b, this angle steadily diminishes from almost 80° in the case where the aryl groups are directly connected to each other (bridge size 0) to 0° in the case of an acyclic derivative. It is also clear that the activation barrier for functionalization correlates with this angle, i.e., the larger α , the higher the functionalization barrier. Apparently, there must be a force present that directs the reaction through a planar pathway as long as sterically possible (vide infra).

In contrast, the arene coupling reaction is not as clearly dependent on geometrical features. There is, however, experimental evidence for a slight preference of the arene coupling reaction in the case of a seven-membered ring.⁶ The calculations show that, in this particular case, the striking difference lies in a boat-like conformation of the transition state, which is readily accessible for a seven-membered ring structure (Figure 5). However, the arene coupling process appears to be feasible only if the equilibrium structure is already disturbed by strain (vide infra).

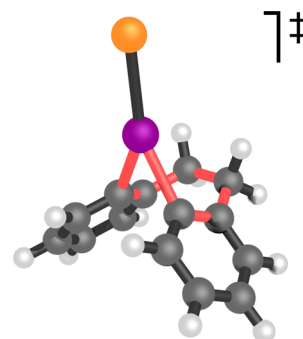
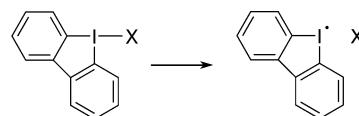


Figure 5. Boat-type TS geometry of the arene coupling reaction of bridged ($n = 2$) bromo diaryliodane (also, see Figure 4a).

On the basis of the experimental observation in strained systems and at low temperatures that only products of radical processes are found, Grushin proposed a single-electron transfer (SET) mechanism for the reaction.⁶ Another possibility for a radical mechanism is the homolytic cleavage of the nucleophile–iodine bond (Scheme 5). In both cases, a cyclic diaryliodine radical is the resulting intermediate. The cleavage of the three-center bond can be induced by thermal population of the lowest-excited states, i.e., an internal dissociative electron transfer (DET).

Scheme 5. Homolytic Cleavage of the Three-Center Bond Resulting in a Diaryliodine and a Nucleophile Radical



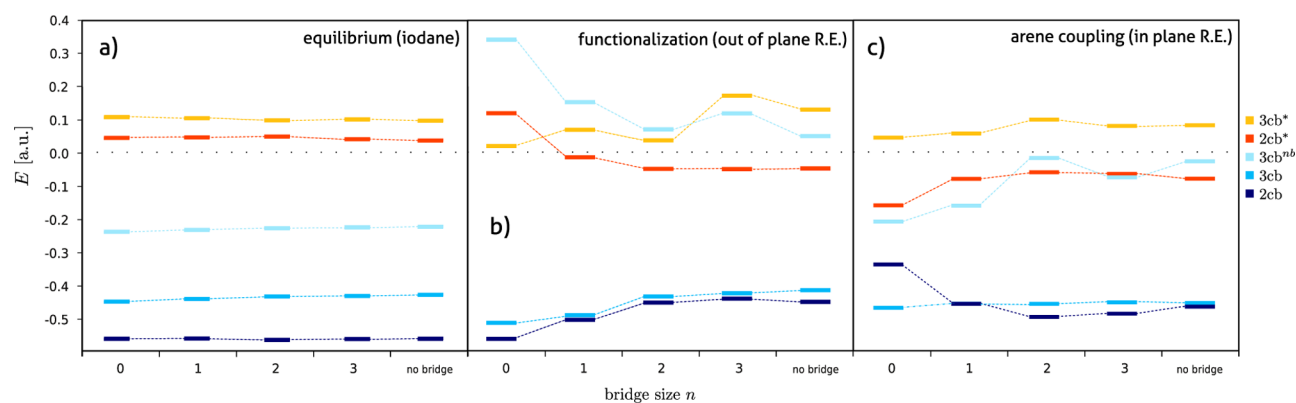


Figure 6. Frontier NLMOs energies of the bridged phenyl diaryliodanes. (a) The increase of the bridge size n has no substantial impact on the electronic structure of the equilibrium geometries. This is obviously not the case for the transition states of both RE reactions (b, c), where the orbital energies change significantly.

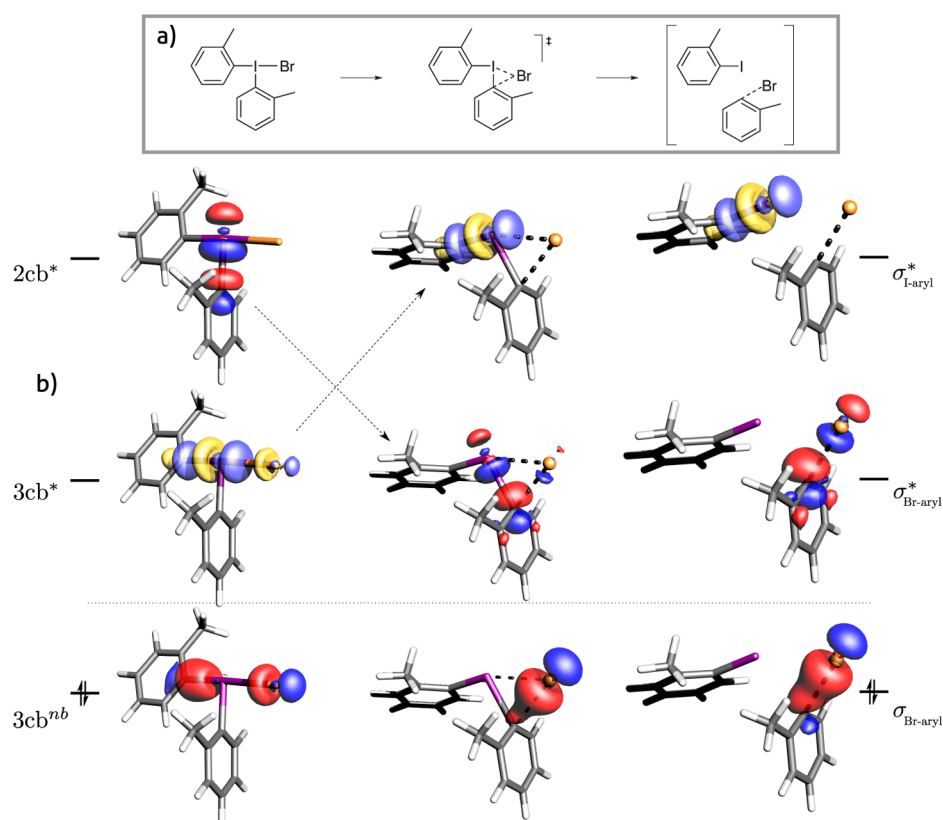


Figure 7. (a) Schematic representation of the RE reaction process of bromine diaryliodane. (b) The frontier NLMOs of bromine diaryliodane in the course of the RE reaction are displayed to show the evolution of the three- and two-center bonds. In this process, the elimination of the most electron-withdrawing ligand is favored (here, bromine ligand). This process is supported by an initial charge separation (see strong polarization of $3cb^{nb}$ in TS). The final recombination depends on the properties of the aryl ligands as the $2cb^*$ becomes the acceptor orbital. The structure on the rhs is close to the TS and does not represent a stationary point.

To explore this proposed DET mechanism, computations of the excited states of the bridged and unbridged diaryliodanes were performed. These calculations reveal that the main contribution to the lowest excited state corresponds to a triplet excitation from the three-center nonbonding to the two-center antibonding orbital. The optimization of the structure of the triplet excited state shows an elongation of the involved bonds, but a barrierless homolytic cleavage of the three-center bond was observed only for polar compounds. A mechanistic discussion of the DET process will be presented using azo 1,1'-biphenyliodane as an example (vide infra).

Mechanistic Considerations: The Three-Center–Four-Electron Bond Model. To obtain an initial idea of the driving forces behind these processes, the properties of the electronic structure have to be elucidated. The application of the 3c–4e bond model has already proved to be a helpful tool to describe the reactivity of λ^3 -iodane chemistry in a conceptual framework.⁵ Therefore, the relevant aspects of the electronic structure of the different diaryliodanes will be expressed by means of a natural bond orbital (NBO) analysis.

In Figure 6, the energies of the frontier natural localized molecular orbitals (NLMOs) of the bridged phenyl diary-

liodanes are depicted as a function of bridge size n . The orbitals are labeled as two-center (2cb) and three-center (3cb) bonds of bonding, nonbonding (nb), or antibonding (*) character. Both RE transition states show noticeable variations of the orbital energies in response to ring size. In stark contrast, the orbital energies of the equilibrium structures remain nearly constant.

From a conceptual point of view, the reductive elimination reaction can be considered as a heterolytic decomposition followed by an intramolecular nucleophilic attack. During the reaction, two bonds are broken, and a new two-center bond is formed, connecting the nucleophile and an aryl ligand (Figure 7a). This context is illustrated in Figure 7 based on the reaction of bromodiaryliodane.

As most of the action involves the $3cb^{nb}$, $3cb^*$, and $2cb^*$ orbitals, the focus is kept on their evolution along the reaction coordinate. In the TS, the $3cb^{nb}$ HOMO gets polarized against the bromine ligand. The $3cb^*$ orbital, on the other hand, evolves in a complementary fashion: it is polarized on two centers, leaving no amplitude at bromine. Concomitantly, the empty $2cb^*$ is lowered in energy, becoming the new LUMO. Hereon, the HOMO–LUMO interaction, representing the intramolecular nucleophilic attack, induces the breaking of 2cb, and the orbital recombination results in the new Br–Aryl bond (Figure 7b, rhs). To optimize the orbital interaction, the nucleophile may have to distort out-of-plane. This, however, is tied to an energy penalty.

Summarizing, the RE is facilitated by an electron-withdrawing nucleophile, which polarizes the three-center bond, thus supporting the charge separation and hence the heterolytic decomposition.⁵ The efficiency of the subsequent recombination step then essentially depends on the aryl ligand involved in the elimination.¹³ This mechanism is valid for both types of RE reactions, but in arene coupling, the polarization of $3cb^{nb}$ is unfavorable, as the reorganization of charge density is hindered by the trans ligand (i.e., the nucleophile), such as is the case for the example shown in Figure 7b.

With the iodane intermediate as the gateway and thus the starting point for all reaction pathways, we already postulated a dissociative electron transfer (DET) as a possible radical mechanism. From Figure 6, we see that the $3cb^{nb}$ and $2cb^*$ orbitals show no reaction to strain. Accordingly, the excitation energies to the first triplet state, which can be thermally populated, fall within a narrow margin (e.g., 2.46 ± 0.09 eV for the azodiaryliodane series).

The main component of this excitation is a $3cb^{nb} \xrightarrow{T} 2cb^*$ transition, which leads to an elongation of the two-center bond, but not to its homolytic cleavage. The bond that breaks is the three-center bond, releasing an azo radical (Figure 8). This is similar to the three-center bond breaking process illustrated in Figure 7. The diaryliodine radical, which “captured” its electron from $3cb^{nb}$, will be metastable.²⁶

Mechanistic Considerations: The Role of Symmetry.

To obtain a more thorough understanding of some of the phenomena observed, it is useful to study a model system such as IH_3 . At a first glance, one might expect IH_3 to have a trigonal planar D_{3h} (Y-shape) rather than a C_{2v} (T-shape) structure. However, one consequence of high symmetry is degenerate electronic states that may couple to nuclear motion, leading to lower symmetry configurations (Jahn–Teller (JT) and pseudo Jahn–Teller (PJT) effects, respectively).²⁷

Given its 10 valence electron configuration, trigonal planar IH_3 , if distorted along an e' normal mode, will take a T-shape

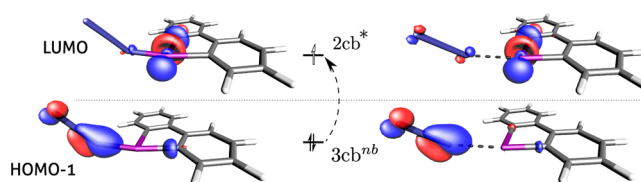


Figure 8. Evolution of the $3cb^{nb}$ and $2cb^*$ NLMOs of azo 1,1'-biphenyl iodane in the course of thermal-induced homolytic decomposition. The optimization of the first excited state results in a distinct elongation of the three-center bond accompanied by a complete polarization of $3cb^{nb}$ toward the azo ligand.

structure that is lower in energy. From Figure 9, it is apparent that the degenerate LUMO splits into $2b_2$ and $4a_1$ components.

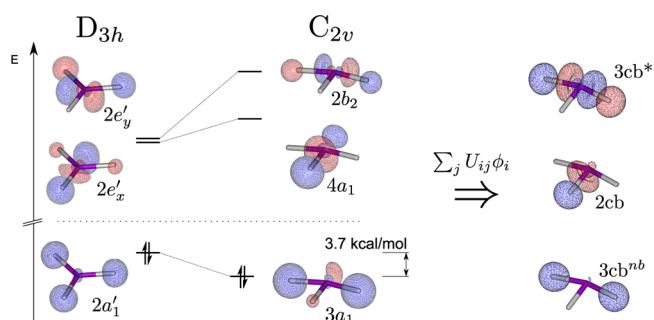


Figure 9. Stabilization of the symmetry broken configuration of IH_3 by a pseudo Jahn–Teller (PJT) effect. The symmetry-induced mixing of the CMOs in the new configuration shifts the s -character from the two-center into the three-center axis, which is emphasized in the 3c–4e bond model (rhs).

The latter will interact with the $3a_1$ HOMO, leading to its stabilization. Another effect of this orbital mixing is the localization of the canonical molecular orbitals (CMOs) along the three- and two-center bonds, respectively. This implies a shift of s -character from the original a'_1 HOMO to the new a_1 LUMO. When localized to NLMOs, these frontier orbitals take the perfect shape of the 3c–4e bond orbitals (Figures 1, rhs, and 9).

The resulting PES is usually described as a “wrapped mexican hat” potential²⁷ with the D_{3h} structure, a second-order saddle point, in its center. At this configuration, for IH_3 , the lowest allowed excited state is indeed of ${}^1E'$ symmetry, dominated by the contribution of the $a'_1 \rightarrow e'$ HOMO–LUMO transition. Located around the center of the PES, three minima are interconnected by isomerization transition states. (In the PES of IH_3 , the isomerization TS is also a second-order saddle point, which is in contrast to IF_3 and presumably also to differently substituted λ^3 -halides. Nevertheless, for the sake of clarity, we will not discuss this issue in the present article.) PJT effects have also been observed in computational studies on halogen trifluorides (XF_3).^{28–30} Overall, the PJT effect is not only responsible for the T-shape equilibrium structure but also leads to the 3c–4e picture.

If, on the other hand, Y-shaped IH_3 is distorted along an a''_2 normal mode, leading to a nonplanar geometry with C_{3v} symmetry, we again observe a PJT effect. In this case, however, the two highest occupied orbitals start mixing (Figure 10), leading to an overall destabilization. This illustrates the energy penalty for a planarity violation in situations where strain forces a nonplanar TS geometry.

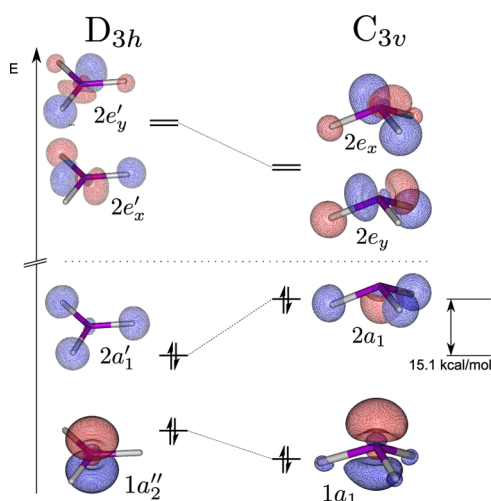


Figure 10. Distortion of the hydrogen ligands of IH_3 out of the molecular plane causes a strong destabilization, due to the unfavorable mixing in the pyramidal configuration involving the lone pair of the iodine center.

With regard to electronic structure, we observe that this distortion transforms the character of the HOMO from a nonbonding to an antibonding orbital, resulting in a destabilization of the HOMO by as much as 15 kcal/mol. In other words, the p_z lone pair $1a_2''$ at the iodine center preserves the planarity of IH_3 , contributing to unfavorable orbital mixing in the case of this out-of-plane distortion.

Again, additional evidence for the presence of PJT coupling is provided by inspecting single-electron transitions. In this case, the transition of interest involves the HOMO and the virtual $6p_z$ orbital (which has equivalent symmetry as that of HOMO-1): $a_1' \rightarrow a_2''$. Even though it contributes to a high-lying excited state, it marks the first allowed spin singlet. In the out-of-plane C_{3v} configuration, the oscillator strength of this excitation increases significantly, pointing to an enhancement of the coupling to the a_2'' bending mode.

Exploring the RE reactions with the IH_3 model from an orbital symmetry perspective allows us to understand some

additional mechanistic details.^{31,32} We have seen that both RE reactions, functionalization and arene coupling, are mechanistically similar, but they display different TS geometries. For functionalization reactions, a bent TS geometry is observed, whereas a Y-shaped symmetric TS geometry is observed only in the case of arene coupling. This TS, however, has a higher barrier that appears to be incompatible with Grushin's proposition, which states that all RE reactions have to pass through a Y-shaped configuration in order to be symmetry-allowed.

We address this issue with our model system by following the reactions starting from T-shaped (C_{2v}) and Y-shaped (D_{3h}) configurations (Figure 11a). The orbitals and orbital energies shown are obtained from constrained scans along the reaction coordinates of the two RE processes. In both cases, we imposed the least deviation from the starting geometry and thus did not strictly follow the lowest-energy pathway. For the elimination starting from the C_{2v} configuration, a perpendicular arrangement of two of the ligands was imposed along the entire reaction coordinate. Analogously, the C_2 axis was chosen as a constrain for the reaction pathway starting from the D_{3h} configuration.

Looking at the evolution of the CMOs, the striking fact is the observation of the crossing of an occupied and unoccupied level for the RE starting from a C_{2v} configuration (Figure 11b), indicating a symmetry-forbidden reaction. On the other hand, starting from the Y-shaped configuration, there is no crossing of occupied and empty levels, which would correspond to a symmetry-allowed mechanism (Figure 11c). However, it should be noted that the D_{3h} starting configuration (actually, a saddle-point of IH_3 connecting the C_{2v} configurations) is much higher in energy and that, therefore, the reaction pathway is unlikely to pass through this Y-shaped configuration.

It turns out that Grushin's criterion of a Y-shaped conformation is sufficient, but not necessary, for a symmetry-allowed reaction. In order for the symmetry-allowed RE reaction to take place, the initial symmetry of the T-shaped equilibrium structure has to be broken. As a matter of fact, inspection of the unconstrained reaction pathway reveals a deviation of the perpendicular arrangement, resulting in an unsymmetrical bent Y-shaped transition structure (Figure 12b).

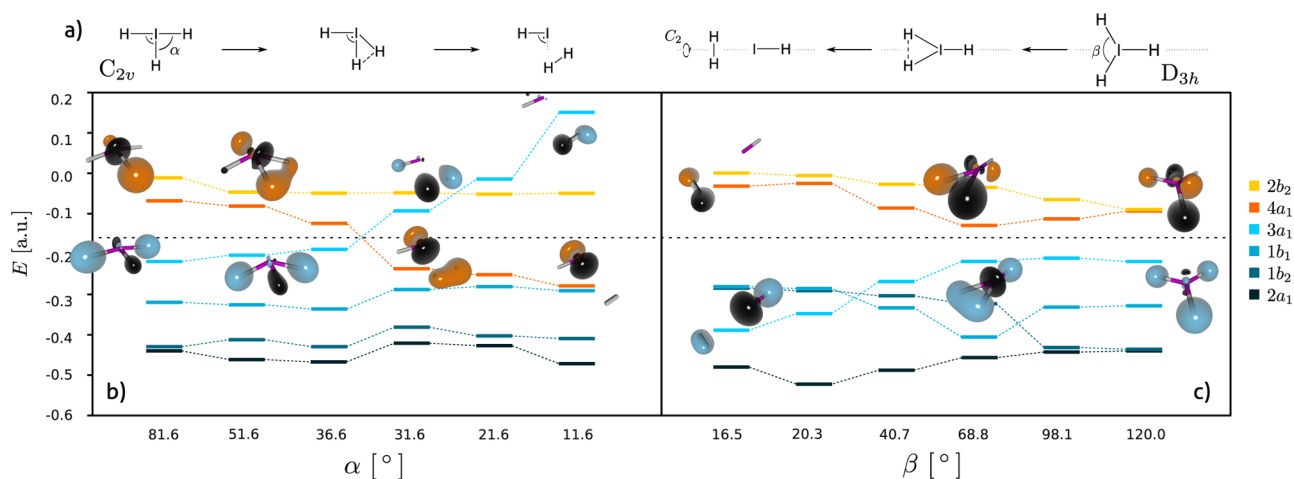


Figure 11. (a) Schematic representation of RE with IH_3 . (b, c) Walsh diagrams of the elimination reaction of H_2 in the model system IH_3 starting from different configurations resulting in a symmetry-forbidden (b) or a symmetry-allowed reaction path (c). The orbitals are labeled according the C_{2v} configuration, and blue shaded orbital energies correspond to initially occupied orbitals. In addition, the evolution of the HOMO ($3a_1$) and LUMO ($4a_1$) is displayed along the reaction coordinates α and β .

At the same time, an orbital level crossing is avoided. This bent geometry is found for the RE transition structures of λ^3 -iodanes in general.

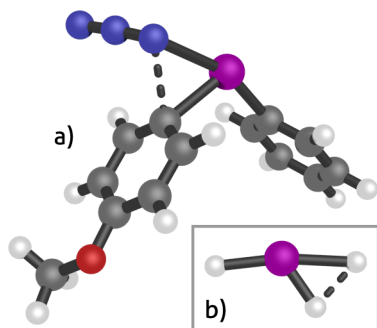


Figure 12. Comparison of the RE TS structures of azo-4-methoxyaryl-phenyl-iodane (a) and IH_3 (b), both showing a bent Y-shaped geometry. Note that the IH_3 TS structure is, unlike that in Figure 11, from an unconstrained scan.

The direction of the functionalization reactions is actually determined by the electronic properties of the ligands, with electron-withdrawing ligands being preferably involved in the elimination process (Figure 12a).⁵ The situation changes if the less electron-withdrawing ligands are to be eliminated. In this case, much more energy is needed to overcome the reaction barrier. The most extreme situation is represented by the arene coupling reaction, in which the elimination of the corresponding ligands is such an unfavorable process that as much symmetry allowance as possible is incorporated. The result is a symmetrical TS geometry with a relatively high, and therefore not competitive, reaction barrier.

CONCLUSIONS

Our computational investigation shows that the structural and electronic properties of the iodanes, species formed in situ as intermediates from the reaction of diaryliodonium salts with a nucleophile, are crucial to their reactivity. In particular, we have shown that these iodanes govern reactivity and also act as a “gateway” to direct the reaction either toward reductive elimination or a radical process, thereby possibly leading to a variety of products. Finally, these T-shaped iodanes undergo rapid isomerization via a Y-shaped transition structure, a process driven by a pseudo Jahn–Teller effect.

However, structural constraints will take effect on the basic course of the reaction. If the aryl ligands bound to the iodine center are bridged, then the strain on the hypervalent region will have an essential impact on the electronic landscape. In contrast, for unstrained systems, functionalization will be favored, and we observe arene coupling and radical mechanisms for moderately or strongly strained systems.

In the case of very strained systems, the reaction is forced toward a homolytic decomposition, as this is the only mechanism that is not influenced by the strain of the hypervalent region. The excitation energy for the thermally induced transition from the 3cb^{nb} orbital to the 2cb^* orbital was shown to be approximately constant within a given series of bridged diaryliodonanes. The analysis of the frontier molecular orbitals nicely explains the mechanism of the homolytic cleavage of the three-center bond.

Even though we observe different TS geometries for the RE mechanisms, both reactions are following a symmetry-allowed

pathway starting from the T-shaped equilibrium structure. Without strain, in this case, the actual height of the reaction barriers depend on the ligands involved in the elimination step. Reductive elimination will most often lead to functionalization rather than arene coupling.

However, the retention of planarity is essential. Deviation from planarity leads to higher barriers, as illustrated for the functionalization reaction involving bridged diaryliodonanes. The energy penalty in such cases was shown to be related to an unfavorable interaction involving the iodine lone pair, which again can be related to a PJT effect.

Finally, breaking down the reactivity of λ^3 -iodanes has revealed that the hypervalent moiety is responsible for the versatile chemistry of iodanes. It is the electronic configuration of λ^3 -iodanes that makes the reagents susceptible to a PJT effect. The consequence is the establishment of a $3\text{c}-4\text{e}$ bond and thus the occurrence of nonequivalent bonds. This enables λ^3 -iodanes to isomerize and react along unusual reaction patterns, in stark contrast to other hypervalent molecules, which are not affected by the PJT effect.

ASSOCIATED CONTENT

Supporting Information

Additional material on the calculations as well as the Cartesian coordinates of all compounds. This material is available free of charge via the Internet at <http://pubs.acs.org>.

AUTHOR INFORMATION

Corresponding Author

*E-mail: hans.luethi@phys.chem.ethz.ch.

Notes

The authors declare no competing financial interest.

ACKNOWLEDGMENTS

This research was supported by the Swiss National Science Foundation (SNF) and has greatly benefited from discussions with Peter Schwerdtfeger.

REFERENCES

- Zhdankin, V. V. *Hypervalent Iodine Chemistry: Preparation, Structure, and Synthetic Applications of Polyvalent Iodine Compounds*; John Wiley & Sons: Chichester, UK, 2013.
- Zhdankin, V. V.; Stang, P. *Chem. Rev.* **2008**, *108*, 5299–5358.
- Hypervalent Iodine Chemistry: Modern Developments in Organic Synthesis*; Wirth, T., Ed.; Springer: Berlin, 2003; Vol. 224.
- Merritt, E. A.; Olofsson, B. *Angew. Chem., Int. Ed.* **2009**, *48*, 9052–9070.
- Pinto de Magalhães, H.; Lüthi, H. P.; Togni, A. *Org. Lett.* **2012**, *14*, 3830–3833.
- Grushin, V. V. *Chem. Soc. Rev.* **2000**, *29*, 315–324.
- Chemistry of Hypervalent Compounds*; Akiba, K.-y., Ed.; Wiley-VCH: New York, 1999.
- Musher, J. *Angew. Chem., Int. Ed. Engl.* **1969**, *8*, 54–68.
- Ponec, R.; Duben, A. J. *J. Comput. Chem.* **1999**, *20*, 760–771.
- Ponec, R.; Yuzhakov, G.; Cooper, D. L. *Theor. Chem. Acc.* **2004**, *112*, 419–430.
- Woon, D. E.; Dunning, T. H., Jr. *Comput. Theor. Chem.* **2011**, *963*, 7–12.
- Moss, R. A.; Wilk, B.; Krogh-Jespersen, K.; Blair, J. T.; Westbrook, J. D. *J. Am. Chem. Soc.* **1989**, *111*, 250–258.
- Malmgren, J.; Santoro, S.; Jalalian, N.; Himo, F.; Olofsson, B. *Chem.—Eur. J.* **2013**, *19*, 10334–10342.
- Wang, B.; Graskemper, J. W.; Qin, L.; DiMagno, S. G. *Angew. Chem., Int. Ed.* **2010**, *49*, 4079–4083.

- (15) Frisch, M. J. et al. *Gaussian 09*, Revision A.02; Gaussian Inc.: Wallingford, CT, 2009.
- (16) Glendening, E. D.; Reed, A. E.; Carpenter, J. E.; Weinhold, F. *NBO*, version 3.1, 1988.
- (17) Becke, A. J. *Chem. Phys.* **1993**, 5648–5652.
- (18) Lee, C.; Yang, W.; Parr, R. *Phys. Rev. B* **1988**, 785–789.
- (19) Vosko, S.; Wilk, L.; Nusair, M. *Can. J. Phys.* **1980**, 1200–1211.
- (20) Stephens, P.; Devlin, F.; Chabalowski, C.; Frisch, M. J. *Phys. Chem.* **1994**, 11623–11627.
- (21) Dunning, T. J. *Chem. Phys.* **1989**, 1007.
- (22) Peterson, K. A.; Shepler, B. C.; Figgen, D.; Stoll, H. *J. Phys. Chem. A* **2006**, 13877.
- (23) Furche, F.; Ahlrichs, R. *J. Chem. Phys.* **2002**, 117, 7433–7447.
- (24) Scalmani, G.; Frisch, M. J.; Mennucci, B.; Tomasi, J.; Cammi, R.; Barone, V. *J. Chem. Phys.* **2006**, 124, 094107.
- (25) Caricato, M.; Mennucci, B.; Tomasi, J.; Ingrosso, F.; Cammi, R.; Corni, S.; Scalmani, G. *J. Chem. Phys.* **2006**, 124520.
- (26) Razskazovskii, Y. V.; Raiti, M. J.; Sevilla, M. D. *J. Phys. Chem. A* **1999**, 103, 6351–6359.
- (27) Bersuker, I. B. *Chem. Rev.* **2001**, 101, 1067–114.
- (28) Yang, D.-D.; Wang, F. *Phys. Chem. Chem. Phys.* **2012**, 14, 15816–15825.
- (29) Schwerdtfeger, P. *J. Phys. Chem.* **1996**, 100, 2968–2973.
- (30) Kim, H.; Choi, Y. J.; Lee, Y. S. *J. Phys. Chem. B* **2008**, 112, 16021–16029.
- (31) Bachler, V.; Halevi, E. A. *Theor. Chim. Acta* **1981**, 59, 595–602.
- (32) Falceto, A.; Casanova, D.; Alemany, P.; Alvarez, S. *Inorg. Chem.* **2013**, 52, 6510–6519.